Journal of Solid State Chemistry 182 (2009) 413–420

Contents lists available at ScienceDirect

Journal of Solid State Chemistry

journal homepage: www.elsevier.com/locate/jssc

New open-framework in the uranyl vanadates $A_3(UO_2)_7(VO_4)_5O$ (A = Li, Ag) with intergrowth structure between $A(UO_2)_4(VO_4)_3$ and $A_2(UO_2)_3(VO_4)_2O$

S. Obbade *, C. Renard, F. Abraham

Unité de Catalyse et de Chimie du Solide, UCCS UMR CNRS 8181, ENSCL-USTL, B.P. 90108, 59652 Villeneuve d'Ascq Cedex, France

ARTICLE INFO

Article history:
Received 22 July 2008
Received in revised form
29 September 2008
Accepted 12 October 2008
Available online 29 October 2008

Keywords:
Uranyl vanadate
Crystal structure determination
Solid-state synthesis
Intergrowth structure
Cationic conductivity

ABSTRACT

New uranyl vanadates $A_3(UO_2)_7(VO_4)_5O$ (M = Li (**1**), Na (**2**), Ag (**3**)) have been synthesized by solid-state reaction and their structures determined from single-crystal X-ray diffraction data for **1** and **3**. The tetragonal structure results of an alternation of two types of sheets denoted S for $^2_\infty[UO_2(VO_4)_2]^{4-}$ and D for $^2_\infty[(UO_2)_2(VO_4)_3]^{5-}$ built from UO_6 square bipyramids and connected through VO_4 tetrahedra to $^1_\infty[U(3)O_5\text{-}U(4)O_5]^{8-}$ infinite chains of edge-shared $U(3)O_7$ and $U(4)O_7$ pentagonal bipyramids alternatively parallel to a- and b-axis to construct a three-dimensional uranyl vanadate arrangement. It is noticeable that similar $_\infty[UO_5]^{4-}$ chains are connected only by S-type sheets in $A_2(UO_2)_3(VO_4)_2O$ and by D-type sheets in $A(UO_2)_4(VO_4)_3$, thus $A_3(UO_2)_7(VO_4)_5O$ appears as an intergrowth structure between the two previously reported series. The mobility of the monovalent ion in the mutually perpendicular channels created in the three-dimensional arrangement is correlated to the occupation rate of the sites and by the geometry of the different sites occupied by either Na, Ag or Li. Crystallographic data: 293 K, Bruker X8-APEX2 X-ray diffractometer equipped with a 4 K CCD detector, Mo$K\alpha$, $\lambda = 0.71073$ Å, tetragonal symmetry, space group $P\bar{4}m2$, $Z = 1$, full-matrix least-squares refinement on the basis of F^2; **1**, $a = 7.2794(9)$ Å, $c = 14.514(4)$ Å, R1 = 0.021 and wR2 = 0.048 for 62 parameters with 782 independent reflections with $I \geqslant 2\sigma(I)$; **3**, $a = 7.2373(3)$ Å, $c = 14.7973(15)$ Å, R1 = 0.041 and wR2 = 0.085 for 60 parameters with 1066 independent reflections with $I \geqslant 2\sigma(I)$.

1. Introduction

In recent years, the study of structural arrangements of uranyl polyhedra and inorganic oxoanions such as silicate, phosphate, arsenate, vanadate, molybdate, tungstate… has led to a rapidly expanding group of compounds, whose structures are dominated by the formation of two-dimensional (2-D) topologies [1,2]. The structural diversity of these compounds is related to (1) the variety of coordination polyhedra about U(VI) (hexagonal, pentagonal or rectangular bipyramid), (2) the various geometries of the inorganic oxoanions (tetrahedron, square pyramid, octahedron…) centered on post-transition elements (Si, P, As) or transition metals in their highest possible oxidation states (V, Nb, Mo, W, etc.) and (3) the huge possibilities of direct linkages between uranyl polyhedra or between oxoanions and indirect linkages of uranyl polyhedra through oxoanions. Among the different transition metal-centered oxoanions, the vanadium ion is particularly interesting since the coordination of V^{5+} in uranyl-containing oxides is either a square pyramid or a tetrahedron and the uranyl vanadates family magnificently illustrates the variety of coordination geometries and the flexibility of the association between polyhedra. When V^{5+} occurs in square pyramids, the vanadyl V═O bonds are parallel to the uranyl ions and preclude the association of polyhedra in the direction of these linear entities leading to 2-D arrangements as in the carnotite-type compounds $A_2(UO_2)_2(V_2O_8)$ [3–6] and in $CsUV_3O_{11}$ [7], the alkali metals occupying the interspace between the anionic layers. When V^{5+} is in tetrahedral coordination, there is still a tendency to layered structures such as in $A_6[(UO_2)_5(VO_4)_2]O_5]$ with A = Na, K, Rb [8,9], in $A_7[(UO_2)_8(VO_4)_2]O_8Cl]$ with A = Rb, Cs [10], and in $Cs_4U_2V_2O_{13}$ [11]. However, using the smallest A^+ ions (Li^+ and Na^+) 3-D arrangements have been obtained in the $A(UO_2)_4(VO_4)_3$ [12] and $A_2(UO_2)_3(VO_4)_2O$ [13] compounds, exemplifying the key role of the counter ions on the obtained uranyl-vanadate architecture. In these two series, the crystal structures are built from zig-zag infinite chains $^1_\infty[UO_5]^{4-}$ of edge-shared UO_7 pentagonal bipyramids further connected through layers $^2_\infty[(UO_2)_2(VO_4)_3]^{5-}$ (noted throughout this paper D), and $^2_\infty[(UO_2)(VO_4)_2]^{4-}$ (noted throughout this paper S), respectively, constituted of VO_4 tetrahedra and UO6 square pyramids. The linkage between the uranium chains and the uranium–vanadium sheets creates open-frameworks with non-crossing channels occupied by the alkaline metals. The

* Corresponding author. Fax: +33 3 20 43 68 14.
E-mail address: said.obbade@ensc-lille.fr (S. Obbade).

0022-4596/$ - see front matter Crown Copyright © 2008 Published by Elsevier Inc. All rights reserved.
doi:10.1016/j.jssc.2008.10.019

differences in the cationic conductivity of the Li and Na-compounds were correlated to the occupation of different sites within the channels by the alkaline metal in the structure of $Na(UO_2)_4(VO_4)_3$ [12] and $Li_2(UO_2)_3(VO_4)_2O$ [13], assuming that Li and Na occupies the same sites in the two series.

The S and D layers are derived from the autunite-type sheet anion topology, their dimensions are similar and they play the same role in the connection of the $^1_\infty[UO_5]^{4-}$ chains, so structures containing both S and D layers can be imagined. This paper describes the synthesis of such compounds where S and D layers alternate (S–D compounds) leading to the formula equal to the sum of the two previously reported compounds containing S layers only (S–S compounds) and D layers only (D–D compounds), that is $A_3(UO_2)_7(VO_4)_5O$ obtained for A = Li (**1**), Na(**2**) and Ag(**3**). The crystal structures of **1** and **3** determined from single crystal X-ray diffraction confirm that Li and Ag occupy different sites within the channels.

2. Experimental

2.1. Synthesis

Tries of synthesis of $A_3(UO_2)_7(VO_4)_5O$ ($A_3U_7V_5O_{35}$) powders have been accomplished for A = Li, Na, Ag by solid-state reactions between uranyl nitrates, $(UO_2)(NO_3)_2\cdot 6H_2O$ (Merck), monovalent cation carbonates, A_2CO_3 (Aldrich) and vanadium oxide, V_2O_5 (Aldrich).

Homogeneous mixtures of the initial materials according to the reaction $3/2A_2CO_3+7(UO_2)(NO_3)_2\cdot 6H_2O+5/2V_2O_5 \rightarrow A_3U_7V_5O_{35}+3/2CO_2+14NO_2+42H_2O+7/2O_2$ were heated to 500 °C for 12 h and then up to 750 °C, in platinum crucibles, and maintained at this temperature during 1 week and finally cooled to room temperature, with intermediate grindings after each cooling.

With the aim to prepare single crystals, the resulting powders were melted at 950 °C (A = Li), 950 °C (A = Na) and 900 °C (A = Ag) and cooled at the rate of 5 °C/h to 700 °C and finally at 15 °C/h to room temperature. For A = Li well-developed yellow single crystals of **1** were obtained. For A = Na, the resulting sample was a mixture of two types of single crystals corresponding to the carnotite-type compound $Na_2(UO_2)_2(V_2O_8)$ [5] and to the D–D compound $Na(UO_2)_4(VO_4)_3$ [12]. Finally for A = Ag, the resulting sample was a mixture of single crystals of the carnotite-type compound $Ag_2(UO_2)_2(V_2O_8)$ [6] and $U_2V_2O_{11}$ [14,15] accompanied by U_3O_8 powder. Single crystals of **3** were obtained by melting the powder corresponding to the stoechiometry of the expected $Ag_2(UO_2)_3(VO_4)_2O$ (D–D compound) during fruitless tries of synthesis of this compound.

The unit cell parameters were refined by using the same method as for $Li_2(UO_2)_3(VO_4)_2O$ [13] from the powder diffraction patterns recorded at room temperature, using a D8 Advance diffractometer (Bruker AXS, Germany) with Bragg Brentano θ/θ geometry (40 kV, 40 mA) and Cu$K\alpha$ radiation with secondary graphite monochromator. The powder diagrams were recorded with steps of 0.02° and a counting time of 15 s per step, within an angular range of 5–80° in 2θ .

The density of **3** prepared as pure powder was measured with an automated Micromeritics Accupy 1330 helium pycnometer using a 1-cm^3 cell.

2.2. Single-crystal X-ray diffraction and structure determination

For **1** and **3**, a well-shaped yellow crystal was selected for X-ray diffraction investigations. The measurement of X-ray intensities was performed at room temperature using a Bruker X8-APEX2 X-ray diffractometer, equipped with a 4 K CCD detector and monochromatic Mo$K\alpha$ radiation (λ = 0.7107 Å). Details of the data collection are given in Table 1. Before the crystal structure determination, intensity data were corrected for Lorentz polarization and background effects using the SAINT-Plus 7.12 software package [16]. Then the absorption corrections were computed by a semi-empirical method based on redundancy, using the SADABS 2006/1 program [17,18]. The crystal structures of **1** and **3** were solved in the non-centrosymmetric $P\bar{4}m2$ space group, by means of direct methods strategy using SHELXS program [19] that localize the heavy atoms, U, V and Ag. The positions of the oxygen and Li atoms were deduced from subsequent refinements and difference Fourier syntheses. The atomic scattering factors for neutral atoms were taken from the "International Tables for X-ray Crystallography" [20]. The final refinements included anisotropic displacement parameters for U, V and Ag and isotropic displacements parameters for O and Li atoms. The atomic coordinates and isotropic displacement parameters are listed in Table 2. The most significant metal to oxygen distances with bond valences and uranyl angles are reported in Table 3. Bond valences were calculated using Brese and O'Keeffe data [21] with b = 0.37 Å except for U–O bonds the coordination independent parameters (R_{ij} = 2.051 Å, b = 0.519 Å) were taken from Burns et al. [22].

Table 1
Crystal data, intensity collection and structure refinement parameters for $A_3U_7V_5O_{35}$, A = Li, Ag..

	$Li_3U_7V_5O_{35}$,	$Ag_3U_7V_5O_{35}$,
Crystal data		
Crystal symmetry	Tetragonal	Tetragonal
Space group	$P\bar{4}m2$ (no. 115)	$P\bar{4}m2$ (no. 115)
Chemical formula weight (g mol−1)	2501.73	2804.52
Unit cell	$a = b$ = 7.2794(9) Å	$a = b$ = 7.2373(3) Å
	c = 14.514(4) Å	c = 14.7973(15) Å
	V = 769.1(2) Å^3	V = 775.06(9) Å^3
Z	1	1
Calculated density (g/cm^3)	5.40 (1)	6.01(1)
Data collection		
Temperature (K)	296 (2)	296(2)
Radiation Mo($K\alpha$)	0.71073 Å	0.71073 Å
Scan mode	ω scans	ω scans
Recording angular range (deg.)	3.13–28.98	3.13–29.32
Recording reciprocal space	$-9\leqslant h\leqslant 9$	$-9\leqslant h\leqslant 9$
	$-9\leqslant k\leqslant 9$	$-9\leqslant k\leqslant 9$
	$-19\leqslant l\leqslant 19$	$-20\leqslant l\leqslant 20$
Number of reflexions	4460	5755
R_equivalents:R_{int}	0.0464	0.0577
Measured/independent	782	1066
Absorption μ (cm^{-1})	382.60	398.06
Refinement		
Refined parameters/restraints	62/0	60/0
Goodness of fit on F^2	1.07	1.05
R1[a] [$I>2\sigma(I)$]	0.021	0.041
wR2[b] [$I>2\sigma(I)$]	0.048	0.085
Largest diff. peak and hole (e Å^{-3})	1.332/−1.485	2.353/−2.266

[a] $R1 = \sum(|F_o|-|F_c|)/\sum|F_o|$.
[b] $wR2 = [\sum w(F_o^2-F_c^2)^2/\sum w(F_o^2)^2]^{1/2}$ with $w = 1/[\sigma^2(F_0^2)+(a\,P)^2+b\,P]$ where a and b are refinable parameters and $P = (F_o^2+2F_c^2)/3$.

2.3. Electrical conductivity measurements and thermal analyses

Electrical conductivity measurements were carried out on cylindrical pellets (diameter, 5 mm; thickness, ca. 3 mm) obtained using a conventional cold press and sintered at 750 °C for two

Table 2
Atomic coordinates and isotropic (Li, O atoms) or equivalent (U, V, Ag atoms) displacement parameters for $A_3U_7V_5O_{35}$ with A = Li (first line) and Ag (second line)..

Atom	Site	Occupation	x	y	z	(U_{iso}/U^a_{eq} *)
U1	1*b*	1	1/2	1/2	0	0.0148 (4)*
			1/2	1/2	0	0.0140 (4)*
U2	2*g*	1	1/2	0	0.43218 (5)	0.0086 (3)*
			1/2	0	0.43755 (7)	0.0095 (3)*
U3	2*e*	1	0	0	0.14504 (6)	0.0108 (3)*
			0	0	0.14359 (7)	0.0126 (3)*
U4	2*g*	1	1/2	0	0.72515 (5)	0.0136 (2)*
			1/2	0	0.72600 (7)	0.0138 (3)*
V1	2*e*	1	0	0	0.3711 (2)	0.0103 (7)*
			0	0	0.3685 (3)	0.0107 (8)*
V2	2*g*	1	1/2	0	0.9471 (2)	0.0092 (7)*
			1/2	0	0.9450 (3)	0.0106 (9)*
V3	1*c*	1	1/2	1/2	1/2	0.0278 (9)*
			1/2	1/2	1/2	0.0175 (9)*
O1	1*a*	1	0	0	0	0.009 (4)
			0	0	0	0.009 (6)
O2	4*j*	1	0.800 (2)	0	0.4328 (9)	0.025 (3)
			0.803 (3)	0	0.4348 (14)	0.034 (5)
O3	4*k*	1	1/2	0.814 (2)	0.0159 (8)	0.022 (2)
			1/2	0.807 (3)	0.0069 (17)	0.033 (4)
O4	2*f*	1	1/2	1/2	0.8750 (12)	0.027 (4)
			1/2	1/2	0.8766 (18)	0.021 (5)
O5	4*j*	1	0.325 (2)	0	0.8710 (7)	0.024 (3)
			0.326 (3)	0	0.8682 (15)	0.031 (4)
O6	2*g*	1	1/2	0	0.3084 (11)	0.034 (4)
			1/2	0	0.3163 (14)	0.018 (4)
O7	4*j*	1	0	0.820 (1)	0.2944 (8)	0.020 (2)
			0	0.819 (2)	0.2908 (16)	0.033 (4)
O8	4*k*	1	0.694 (2)	1/2	0.5673 (9)	0.031 (3)
			0.691 (3)	1/2	0.5673 (14)	0.026 (5)
O9	2*g*	1	1/2	0	0.5603 (11)	0.028 (5)
			1/2	0	0.5622 (18)	0.021 (6)
O10	4*k*	1	1/2	0.761 (1)	0.7242 (8)	0.020 (2)
			1/2	0.758 (3)	0.7245 (15)	0.033 (4)
O11	4*j*	1	0.754 (1)	0	0.1497 (8)	0.026 (3)
			0.757 (4)	0	0.1506 (14)	0.037 (5)
Li1	2*f*	0.75	1/2	1/2	0.711 (10)	0.028 (8)
Li2	2*g*	0.75	1/2	0	0.161 (11)	0.039 (9)
Ag	4*k*	0.75	1/2	0.2329(7)	0.2082 (5)	0.0909 (2)*

[a]The U_{eq} values are defined by $U_{eq} = 1/3(\sum_i\sum_j U_{ij}a^*_i a^*_j a_i a_j)$.

days, followed by slow cooling, 5 °C/h, to room temperature. Gold electrodes were vacuum-deposited on both flat surfaces of the pellets. Conductivity measurements were performed by ac impedance spectroscopy over the range 1–10^6 Hz with a Solartron 1170 frequency-response analyzer. Measurements were made at 20 °C intervals over the range 50–720 °C on both heating and cooling. Each set of values was recorded at a given temperature after a 1 h stabilization time.

3. Results and discussion

3.1. Powder syntheses

Pure polycrystalline sample of $Ag_3(UO_2)_7(VO_4)_5O$ was obtained and the unit cell parameters were refined from powder X-ray diffraction pattern using Rietveld method [23,24]. The refinement was carried out using the "*pattern matching*" option of Fullproof program [25], where only the profile parameters (cell dimensions, peak shapes, background, zero point correction and symmetry) have been refined. The peak shape was described by a Pseudo-Voigt function with an asymmetry correction at low angles. In order to describe the angular dependence of the peak full-width at half-maximum (H), the formulation of Caglioti et al. [26] was used: $H2 = U\tan 2\theta + V\tan\theta + W$, where U, V and W parameters were refined in the process. The refinement of the cell parameters led to $a = 7.2373(3)$ Å, $c = 14.7973(15)$ Å, with the following agreement factors: Rp = 3.24, Rwp = 5.21, and $\chi^2 = 1.49$. The Fig. 1, shows the good agreement between observed and calculated powder X-ray diffraction patterns. The measured and calculated densities with one formula per unit cell are in good agreement ($\rho_{mes} = 5.97\ (2)$ g/cm^3, $\rho_{cal} = 6.01(1)$ g/cm^3).

The synthesized powder of $Li_3(UO_2)_7(VO_4)_5O$ and $Na_3(UO_2)_7(VO_4)_5O$ contains a very weak quantity of $Li_2(UO_2)_3(VO_4)_2O$ and an unidentified phase, respectively. The unit cell parameters were refined to $a = 7.2794\ (9)$ Å, $c = 14.514(4)$ Å and $a = 7.2414(2)$ Å, $c = 14.7566(5)$ Å for Li and Na, respectively.

3.2. Crystal structure description

The structure of $A_3(UO_2)_7(VO_4)_5O$ contains UO_2^{2+} uranyl ions, VO_4^{2-} vanadate ions and O^{2-} oxo ions and reveals a 3-D framework, being constructed from U and V centered polyhedra. There are four crystallographically unique uranium atoms, U(1) and U(2) in 2*g* and 1*b* special sites with a square bipyramidal coordination of oxygen atoms, U(3) and U(4) occupying 2*e* and 2*g* special sites are surrounded by seven oxygen atoms forming pentagonal bipyramids. All of these U atoms are found as part of uranyl cations UO_2^{2+} with short U═O bond distances ranging from 1.743(9) to 1.860(16) Å. In the $U(1)O_6$ and $U(2)O_6$ square bipyramids, the uranyl ions are perfectly linear and are completed in the equatorial plane by four O(3) atoms forming a tilted square for U(1) and by two pairs of O(2) and O(8) atoms forming a nearly perfect square for U(2) and giving a $U(2)O_6$ square bipyramids of pseudo-symmetry 4/*mmm*. The equatorial U–O bond distances vary in the range from 2.182 to 2.296 Å with an average value 2.235 Å in agreement with the average bond length of 2.264 Å, standard deviation 0.064 Å calculated by Burns [2] from 54 structures with uranyl square bipyramids. Let us point out that the U(1)–O(3) bond length is significantly longer in the Li compound (2.296(11) Å) than in the Ag compound (2.224(22) Å), as a consequence the U(1) atom is underbonded in **1**. In $U(3)O_7$ and $U(4)O_7$ pentagonal bipyramids with *mm*2 symmetry, the uranyl ions are not perfectly linear with O═U═O angles varying in the range of 173.2(9) to 179.1(4)°. In $U(4)O_7$ the equatorial U(4)–O bond lengths vary in a narrow range from 2.322(15) to 2.471(11) Å with an average value of 2.400 Å, when in $U(3)O_7$ three distinct equatorial U(3)–O bond lengths are observed, short for O(1) (2.105(1) Å in **1**), intermediate for O(5) (2.377(12) Å in **1**) and long for O(7) (2.532(11) Å in **1**) with an average value of 2.345 and 2.389 Å for **1** and **3**, respectively. All the equatorial oxygen atoms of the U polyhedra belong to vanadate ions, except the O(1) atom which is shared between two $U(3)O_7$ pentagonal bipyramids. The increase of the average equatorial U–O bond lengths from UO_6 to UO_7 polyhedra is in agreement with the conclusions of Burns from the analysis of numerous well-refined structures [2]. The calculated bond valence sums for U(3) and U(4) are consistent with the formal valence of U^{6+}.

The three independent vanadium atoms are in tetrahedral environments of oxygen atoms with two different symmetry, *mm*2 for V(1) and V(2) and $\bar{4}2m$ for V(3). Let us point out that the V–O bond lengths are significantly shorter for the $V(2)O_4$ tetrahedron than for V(1) and V(3) giving an overbonding of the corresponding vanadium atom both in **1** and **3** with calculated bond valence sums of 5.5 vu.

The $U(3)O_7$ and $U(4)O_7$ pentagonal bipyramids shared O(5)–O(7) opposite edges to form infinite $^1_\infty[UO_5]^{4-}$ zig-zag uranyl chains (Fig. 2a), running down the *b*-axis at $z\sim\frac{1}{4}$ and down the a axis at $z\sim\frac{3}{4}$. These two chains are further connected by sharing the equatorial O(1) atoms of $U(3)O_7$ polyhedra to form a

Table 3
Interatomic distances (Å), valence bond and uranyl angles (°) in $A_3U_7V_5O_{35}$ with A = Li (first line) and Ag (second line)..

Atoms	Distance	S_{ij}	Atoms	Distance	S_{ij}	Atoms	Distance	S_{ij}
U1—O4[a]	1.814 (17)	1.579	U2—O6	1.797 (16)	1.634	U3—O11[h]	1.796 (9)	1.634
	1.826 (27)	1.531		1.794 (21)	1.653		1.769 (22)	1.718
U1—O4[b]	1.814 (17)	1.579	U2—O9	1.860 (16)	1.448	U3—O11[f]	1.796 (9)	1.634
	1.826 (27)	1.531		1.844 (24)	1.502		1.769 (22)	1.718
U1—O3	2.296 (11)	0.624	U2—O2	2.182 (13)	0.777	U3—O1	2.105 (12)	0.901
	2.224 (22)	0.715		2.193 (22)	0.765		2.125 (12)	0.867
U1—O3[c]	2.296 (11)	0.624	U2—O2[f]	2.182 (13)	0.777	U3—O5[l]	2.377 (12)	0.534
	2.224 (22)	0.715		2.193 (22)	0.765		2.366 (22)	0.544
U1—O3[d]	2.296 (11)	0.624	U2—O8[g]	2.229 (13)	0.710	U3—O5[i]	2.377 (12)	0.534
	2.224 (22)	0.715		2.237 (22)	0.708		2.366 (22)	0.544
U1—O3[e]	2.296 (11)	0.624	U2—O8[a]	2.229 (13)	0.710	U3—O7[k]	2.532 (11)	0.396
	2.224 (22)	0.715		2.237 (22)	0.708		2.543 (19)	0.390
	$\sum S_{ij}$	**5.654**		$\sum S_{ij}$	**6.056**	U3—O7[l]	2.532 (11)	0.396
		5.922			**6.101**		2.543 (19)	0.390
Uranyl angle (deg.)		180	Uranyl angle (deg.)		180.0 (4)	$\sum S_{ij}$		**6.029**
O4-U1-O4		180	O6-U2-O9		180.0 (6)			**6.171**
						Uranyl angle (deg.)		175.7 (7)
						O11-U3-O11		173.2 (9)
U4—O10[c]	1.743 (9)	1.814	V1—O2[f]	1.712 (13)	1.286	V2—O3[n]	1.684 (11)	1.379
	1.759 (22)	1.752		1.731 (22)	1.218		1.670 (22)	1.433
U4—O10[m]	1.743 (9)	1.814	V1—O2[h]	1.710 (13)	1.286	V2—O3[o]	1.684 (11)	1.379
	1.759 (22)	1.752		1.731 (22)	1.218		1.670 (22)	1.433
U4—O7[i]	2.349 (10)	0.563	V1—O7[k]	1.718 (11)	1.286	V2—O5	1.686 (11)	1.379
	2.322 (15)	0.590		1.742 (18)	1.186		1.696 (21)	1.321
U4—O7[m]	2.349 (10)	0.563	V1—O7[l]	1.718 (11)	1.286	V2—O5[f]	1.686 (11)	1.379
	2.322 (15)	0.590		1.742 (18)	1.186		1.696 (21)	1.321
U4—O9	2.393 (16)	0.517		$\sum S_{ij}$	**5.088**		$\sum S_{ij}$	**5.502**
	2.424 (24)	0.491			**4.808**			**5.508**
U4—O5[f]	2.471 (11)	0.446			S_{ij}			
	2.452 (21)	0.464	V3—O8[a]	1.716 (13)	1.265			
U4—O5	2.471 (11)	0.446		1.704 (21)	1.286			
	2.452 (21)	0.464	V3—O8	1.716 (13)	1.265			
	$\sum S_{ij}$	6.163		1.704 (21)	1.286			
		6.103	V3—O8[l]	1.716 (13)	1.265			
Uranyl angle (deg.)		179.1(4)		1.704 (21)	1.286			
O10-U4-O10		178.5(9)	V3—O8[c]	1.716 (13)	1.265			
				1.704 (21)	1.286			
				$\sum S_{ij}$	**5.060**			
					5.144			
Ag—O4[a]	2.305 (16)	0.286						
Ag—O6	2.324 (16)	0.273	Li1—O10	1.907 (17)	0.309	Li2—O11	1.853 (17)	0.353
Ag—O11[f]	2.646 (17)	0.114	Li1—O10[e]	1.907 (17)	0.309	Li2—O11[f]	1.853 (17)	0.353
Ag—O11	2.646 (17)	0.114	Li1—O4	2.380 (15)	0.106	Li2—O6	2.139 (16)	0.155
Ag—O10[a]	2.861 (16)	0.064	Li1—O8[e]	2.518 (12)	0.048	Li2—O3[l]	2.504 (13)	0.062
Ag—O10[j]	2.861 (16)	0.064	Li1—O8	2.518 (12)	0.048	Li2—O3[e]	2.504 (13)	0.062
	$\sum S_{ij}$	**0.915**		$\sum S_{ij}$	**0.820**		$\sum S_{ij}$	**0.985**

Symmetry codes.
[a] $y, 1-x, 1-z$.
[b] $x, y, -1+z$.
[c] $1-x, 1-y, z$.
[d] $1-y, x, -z$.
[e] $y, 1-x, -z$.
[f] $1-x, -y, z$.
[g] $1-y, -1+x, 1-z$.
[h] $-1+x, y, z$.
[i] $y, -x, 1-z$.
[j] $-y, x, 1-z$.
[k] $-x, 1-y, z$.
[l] $x, -1+y, z$.
[m] $1-y, x, 1-z$.
[n] $1-x, 1-y, 1+z$.
[o] $x, -1+y, 1+z$.

bi-dimensional $^{2}_{\infty}[U_6O_{19}]^{2-}$ layer parallel to the (0 0 1) plane (Fig. 2b). This bi-dimensional layer is completed by $U(2)O_6$ square bipyramids which are hung on both sides by sharing the O(9) atoms. Thus, $U(4)O_7$ and $U(2)O_6$ polyhedra are directly connected by the so-called cation–cation interaction in which an oxo oxygen of the $U(2)O_2^{2+}$ uranyl ion is also an equatorial oxygen of the $U(4)O_7$ uranium polyhedra [27] giving an asymmetry of the uranyl ion. The cohesion between the perpendicular $^{1}_{\infty}[UO_5]^{4-}$ chains is reinforced by a $^{2}_{\infty}[(UO_2)(VO_4)_2]^{4-}$ layer (S layer) parallel to the (0 0 1) plane and built from $U(1)O_6$ square bipyramids sharing

their four equatorial oxygen atoms O(3) with V(2)O_4 tetrahedra (Fig. 2c). The O(5)–O(5) edges of the V(2)O_4 tetrahedra are shared with the $^1_\infty[UO_5]^{4-}$ chains forming a bi-dimensional $^2_\infty[U_7V_2O_{35}]^{18-}$ sheet (Fig. 2d). Two successive sheets are overlapped to the one in the other and are connected through V(1)O_4 and V(3)O_4 tetrahedra to build a 3-D framework (Fig. 2e). A V(1)O_4 tetrahedron shares an O(7)–O(7) edge with a U(3)O_7 polyhedron of a $^1_\infty[UO_5]^{4-}$ chain and the two O(2) corners with two U(2)O_6 square bipyramids. A V(3)O_4 tetrahedron shares these four O(8) corners with four U(2)O_6 square bipyramids.

The structure of $A_3(UO_2)_7(VO_4)_5O$ compounds can also be described as 1-D $^1_\infty[UO_5]^{4-}$ uranyl chains, which extend alternately in two perpendicular orientations down the $\vec{a}$- and $\vec{b}$-axis and connected by two types of uranyl-vanadate sheets $^2_\infty[(UO_2)(VO_4)_2]^{4-}$ (denoted S) and $^2_\infty[(UO_2)_2(VO_4)_3]^{5-}$ (denoted D) parallel to the (0 0 1) plane, these two sheets alternate along the [0 0 1] direction (Fig. 3f). They have the autunite sheet anion topology [1,2] (Fig. 3a) described on the basis of the {4.4.4.4} graph using the Krivovichev notation [28]. The autunite-type sheet is formed by uranyl square bipyramids and tetrahedra that are connected by sharing vertices (Fig. 3b), each tetrahedron shares its four vertices with four bipyramids and are not available to create a 3-D framework, so the large family of compounds that contains this sheet, with either phosphate or arsenate tetrahedra, are 2-D [29–39]. It is noticeable that, except recently published diamines templated compounds [40], layered uranyl vanadates are not built from autunite-type sheets but from sheets based on the Francevillite anion-topology containing vanadium in square pyramidal coordination [3–6,41–45]. In the S layers (Fig. 3c), half the uranyl square bipyramids are removed so vanadium tetrahedral edges, parallel to the [1 0 0] direction above the mean plane of the sheet and the [0 1 0] direction below, are liberated and can be shared with the $^1_\infty[UO_5]^{4-}$ uranyl chains. The $^1_\infty[UO_5]^{4-}$ chains on both sides of the S layer share their O(1) equatorial oxygen atoms that are located at the center of the squares of the removed uranyl bipyramids. In the D layers (Fig. 3d), half the tetrahedra are removed and two vanadate tetrahedra are attached below and above the empty sites by sharing two vertices with uranyl bipyramids, the non-shared edges being oriented along the [1 0 0] and [0 1 0] directions above and below the sheets, respectively, and allowing the hung on both sides of the sheet of mutually perpendicular $^1_\infty[UO_5]^{4-}$ chains.

Frameworks constructed from mutually perpendicular 1-D $^1_\infty[UO_5]^{4-}$ uranyl chains and linked only either by S layers or by D layers have been recently described in $A_2(UO_2)_3(VO_4)_2O$ [13] and $A(UO_2)_4(VO_4)_3$ [12] compounds denoted S–S (Fig. 3e) and D–D

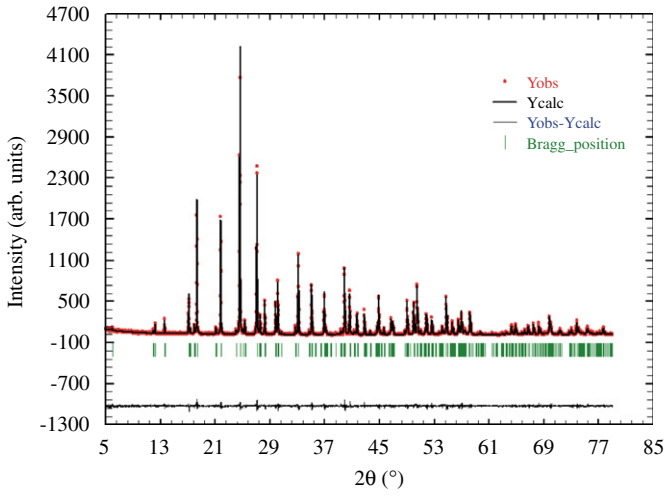

Fig. 1. Observed (Y_{obs}), calculated (Y_{cal}) and difference profiles ((Y_{obs}–Y_{cal}) from Rietveld refinement of X-ray powder diffraction data of $Ag_3(UO_2)_7(VO_4)_5O$. Allowed reflections are indicated by vertical lines.

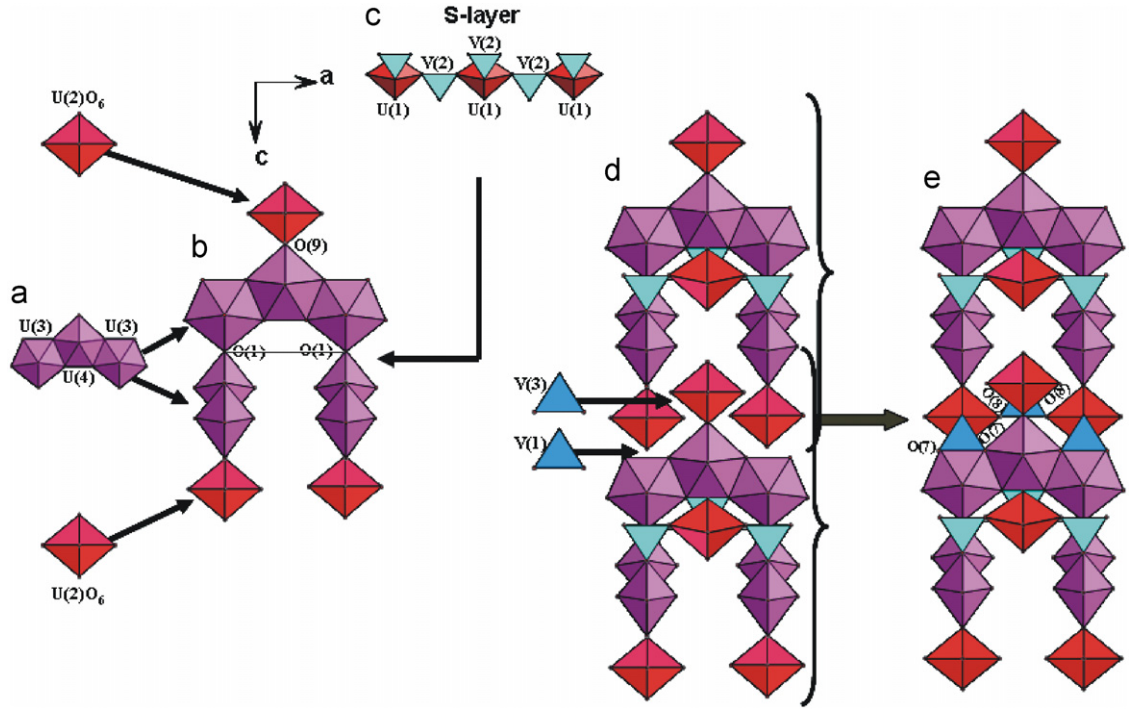

Fig. 2. U(3)O_7 and U(4)O_7 pentagonal bipyramids share opposite equatorial edges to form mono-dimensional $^1_\infty[U(3)U(4)O_{10}]^{8-}$ zig-zag chains (a). Two perpendicular chains are connected by sharing the O(1) equatorial oxygen atom and U(2)O_6 square bipyramids hang on both chains by a cation–cation interaction involving O(9) atoms (b). The cohesion between the perpendicular chains are reinforced by edge sharing with V(2)O_4 tetrahedra that belong to $^2_\infty[(UO_2)(VO_4)_2]^{4-}$ uranyl-vanadates S layers (c). To build thick sheets (d). These sheets parallel to the (0 0 1) plane are connected through $^2_\infty[(UO_2)_2(VO_4)_3]^{5-}$ uranyl-vanadates D layers to create a 3-D uranyl-vanadates framework (e).

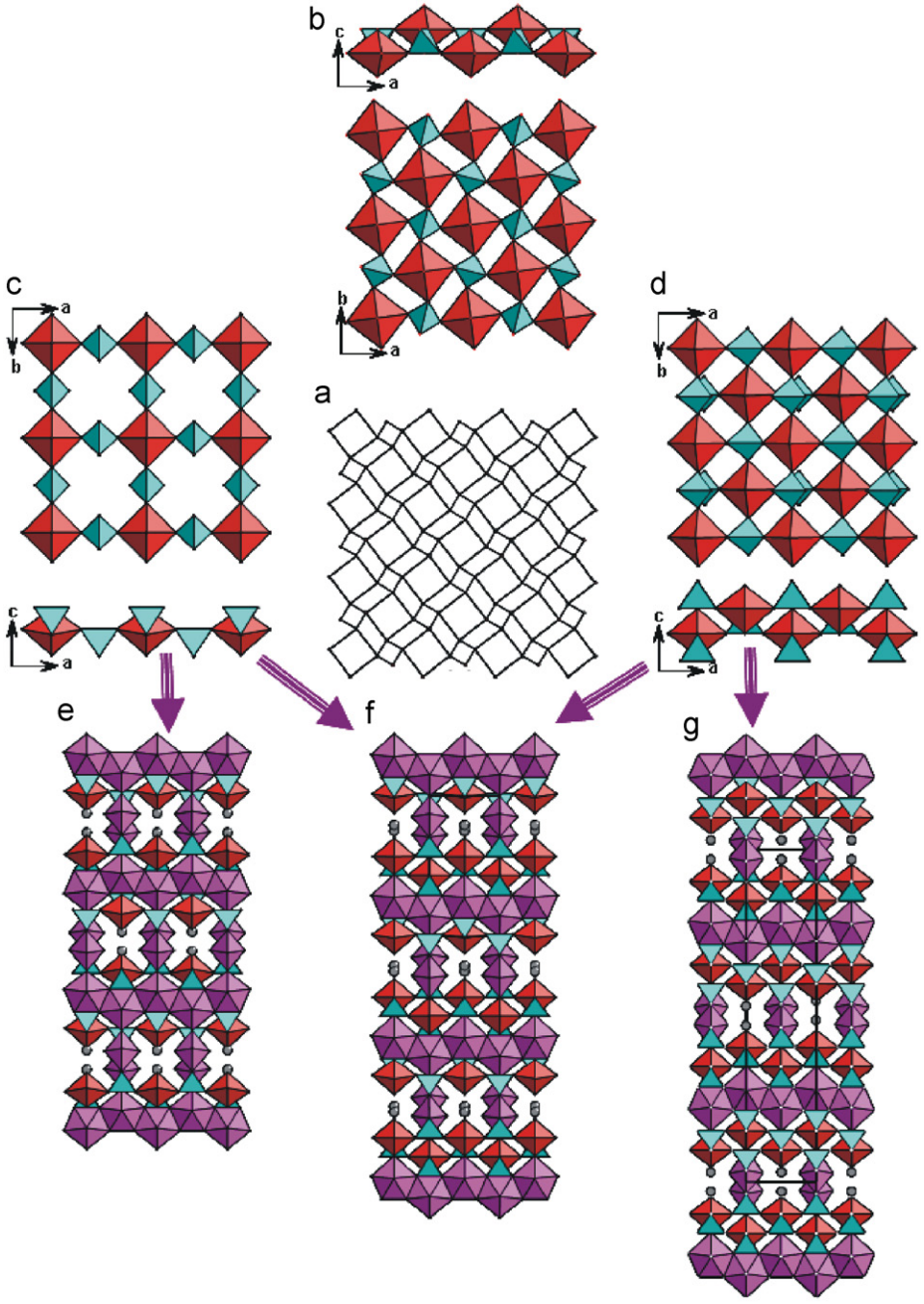

Fig. 3. Different populations of the squares of the autinite sheet anion topology (a) leads to the autunite-type sheet (b) which gives bi-dimensional structures only and to the S (c) and D (d) layers. The arrangements of the $^{1}_{\infty}[UO_5]^{4-}$ chains of edge-sharing UO_7 pentagonal bipyramids and S-type layers only, D-type layers only and S and D layers that alternate lead to the 3-D framework of $A_2(UO_2)_3(VO_4)_2O$ (e); $A(UO_2)_4(VO_4)_3$ (g) and $A_3(UO_2)_7(VO_4)_5O$ (f), respectively.

(Fig. 3g), respectively. Thus, the structure of the present compounds can be considered as a simple S–D intergrowth (Fig. 3f) between the S–S and the D–D series. Considering this description the formula of the various uranyl-vanadate frameworks can be written:

S−S compounds : $\{(UO_2)_2[(UO_2)(VO_4)_2O]\}^{2-}$

D−D compounds : $\{(UO_2)_2[(UO_2)_2(VO_4)_3]\}^{1-}$

S−D compounds : $\{(UO_2)_4[(UO_2)(VO_4)_2O][(UO_2)_2(VO_4)_3]\}^{3-}$

Considering the Na compounds, the value of the c parameter for the S–D compound calculated from those of the S–S and D–D arrangements (and taking into account their body-centered lattice) ($\boldsymbol{c}_{S-D} = (\boldsymbol{c}_{S-S}+\boldsymbol{c}_{D-D})/4 = 14.786$ Å) is in very good agreement with the measured value ($c = 14.7566(5)$ Å).

Whatever the considered framework, similar channels are created running alternately along [1 0 0] and [0 1 0]. The channels are built of face-shared O_6 distorted octahedra, the vertices of the octahedra are uranyl oxygen belonging to two successive UO_7 pentagonal bipyramids of two parallel $^{1}_{\infty}[UO_5]^{4-}$ chains and to two UO_6 square bipyramids (Fig. 4a). For $A = Na$ or Ag, the monovalent ion occupies the center of the octahedra (Fig. 4b). There is one octahedral hole for one UO_7 bipyramid so, for neutrality, the octahedral sites are fully occupied in the S–S compounds, half occupied in the D–D compounds and in three

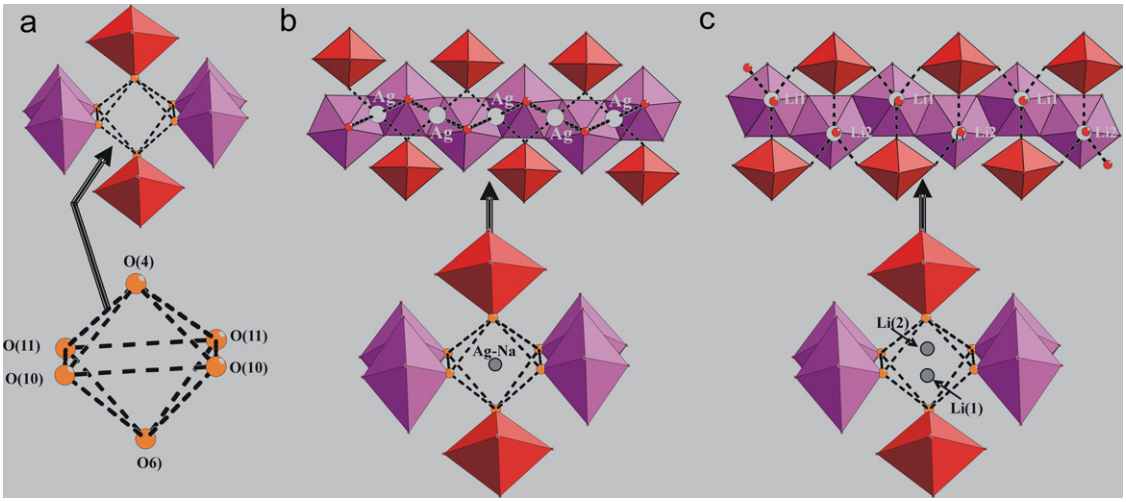

Fig. 4. In $A_3(UO_2)_7(VO_4)_5O$ (A = Li, Na, Ag) compounds the 3-D arrangement of uranium and vanadium polyhedra creates non-crossing 1-D tunnels built from face-sharing of O_6 octahedra and running both down $\vec{a}$- and $\vec{b}$-axis of the tetragonal unit cell (a). The channels are partially populated by Ag^+ ions at the center of the octahedral (b). The Li^+ ions partially occupy the middle of the O(10)–O(10) and O(11)–O(11) edges, for Li(1) and Li(2) respectively, and are surrounded by a trigonal bipyramid of oxygen atoms (c).

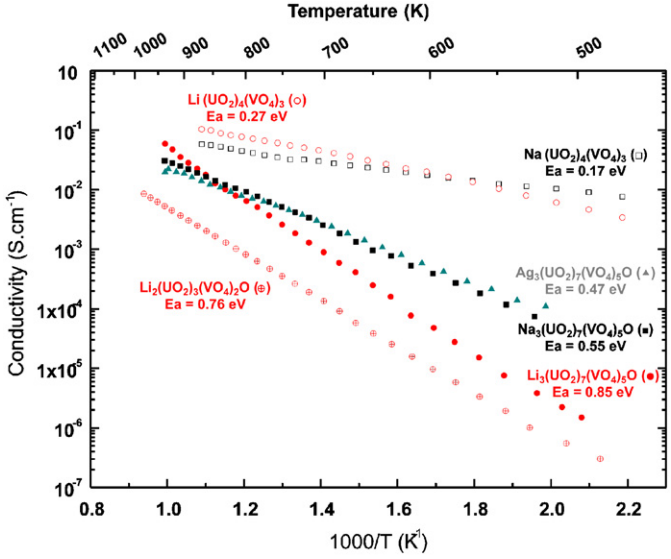

Fig. 5. Conductivity Arrhenius plots for $A_3(UO_2)_7(VO_4)_5O$ (A = Li, Na, Ag) compounds and comparison with $A(UO2)_4(VO_4)_3$ (A = Li, Na) and $Li_2(UO_2)_3(VO_4)_2O$.

quarter in the S–D compounds. In $Li_3(UO_2)_7(VO_4)_5O$, there are two crystallographically unique lithium atoms Li(1) and Li(2) occupying 2*f* and 2*g* sites at the middle of the O(10)–O(10) and O(11)–O(11) edges of the shared octahedral faces, leading to short Li(1)–O(10) and Li(2)–O(11) distances of 1.907(17) and 1.853(17) Å, respectively. The coordination polyhedra around Li atoms are completed by three oxygen atoms at longer distances and appear as trigonal bipyramids (Fig. 4c). The calculated bond valence sums are in good agreement with the formal charge for both Ag and Li. These results confirm the localization of Na (or Ag) and Li in different sites in these types of structures as suggested by crystal structure determination of $Na(UO_2)_4(VO_4)_3$ [12] and $Li_2(UO_2)_3(VO_4)_2O$ [13]. Finally, for oxygen atoms the calculated valence bond sums ranged from 1.685 to 2.352 vu with average values of 2.005 and 2.043 vu for **1** and **3** respectively, showing that the oxygen atoms are only in the ion oxide form.

The alkaline cations mobility in the tunnels has been evidenced by electrical measurements. Thus, the electrical conductivity of the three compounds was measured and is reported in Fig. 5. In spite of the presence of a very weak impurity in Li and Na powders, the results allow some observations. For the three samples an Arrhenius law applies for the whole temperature range explored with a weaker conductivity at low temperature and a higher activation energy for the Li-compound, as already observed in the $A(UO_2)_4(VO_4)_3$ series [12]. The higher activation energy for the Li-compound is correlated to the particular sites occupied by this ion with two short Li–O distances. The conductivities of the S–D series compounds (occupation rate of the cationic sites = 0.75) are between those of the best conductors that belong to the D–D series compounds (occupation rate = 0.50) and the most poor of the S–S series (full occupation).

4. Conclusion

A new series $A_3\square_1\{(UO_2)_4[(UO_2)(VO_4)_2O][(UO_2)_2(VO_4)_3]\}$ with a framework structure has been evidenced for A = Li, Na, Ag. The structure can be described as a simple intergrowth between $A_1\square_1\{(UO_2)_2[(UO_2)(VO_4)_2O]\}$ and $A\{(UO_2)_2[(UO_2)_2(VO_4)_3]\}$ compounds with a succession of S and D layers in the **c**-direction. Other intergrowth structures with more complicated successions of these two types of layers can be imagined but were never observed until today. Synthesis and characterization of similar uranyl phosphates are in progress.

References

[1] P.C. Burns, M.L. Miller, R.C. Ewing, Can. Mineral. 34 (1996) 845.
[2] P.C. Burns, Can. Mineral. 43 (2005) 1839.
[3] D.E. Appleman, H.T. Evans, Am. Mineral. 50 (1965) 825.
[4] P.G. Dickens, G.P. Stuttard, R.G.J. Ball, A.V. Powell, S. Hull, S. Patat, J. Mater. Chem. 2 (1992) 161.
[5] F. Abraham, C. Dion, M. Saadi, J. Mater. Chem. 3 (1993) 459.
[6] F. Abraham, C. Dion, N. Tancret, M. Saadi, Adv. Mater. Res. 1-2 (1994) 511.
[7] I. Duribreux, C. Dion, M. Saadi, F. Abraham, J. Solid State Chem. 146 (1999) 258.
[8] C. Dion, S. Obbade, E. Raekelboom, M. Saadi, F. Abraham, J. Solid State Chem. 155 (2000) 342.
[9] S. Obbade, C. Dion, L. Duvieubourg, M. Saadi, F. Abraham, J. Solid State Chem. 173 (2003) 1.

[10] I. Duribreux, M. Saadi, S. Obbade, C. Dion, F. Abraham, J. Solid State Chem. 172 (2003) 351.
[11] S. Obbade, C. Dion, M. Saadi, F. Abraham, J. Solid State Chem. 177 (2004) 1567.
[12] S. Obbade, C. Dion, M. Rivenet, M. Saadi, F. Abraham, J. Solid State Chem. 177 (2004) 2058.
[13] S. Obbade, L. Duvieubourg, C. Dion, F. Abraham, J. Solid State Chem. 180 (2007) 866.
[14] A.M. Chippinade, P.G. Dickens, G.J. Flynn, G.P. Stuttard, J. Mater. Chem. 5 (1995) 141.
[15] N. Tancret, S. Obbade, F. Abraham, Eur. J. Solid State Inorg. Chem. 32 (1995) 195.
[16] Bruker Analytical X-ray system, Inc., "SAINT Plus, Version 7.12", Madison WI, 2004.
[17] R.H. Blessing, Acta Crystallogr. A51 (1995) 33.
[18] G.M. Scheldrick, SADABS, Bruker-Siemens Area Detector Absorption and Other Correction, Version 2006/1, Goetingen Germany, 2006.
[19] G. M. Sheldrick, SHELX-97, Bruker Analytical X-ray Instruments, Inc., Madison, WI, 1997.
[20] J.A. Ibers, W.C. Hamilton (Eds.), International Tables for X-ray Crystallography, Vol. IV, Kynoch Press, Birmingham, UK, 1974.
[21] N.E. Bresse, M. O'Keeffe, Acta Crystallogr. B47 (1991) 192.
[22] P.C. Burns, R.C. Ewing, F.C. Hawthorne, Can. Mineral. 35 (1997) 1551.
[23] H.M. Rietveld, Acta Crystallogr. 22 (1967) 151.
[24] H.M. Rietveld, Acta Crystallogr. 25 (1992) 589.
[25] J. Rodrigez Carvajal, M.T. Fernandez Diaz, J.L. Martinez, J. Phys.: Condens. Matter 3 (1991) 3215.
[26] C. Caglioti, A. Paoletti, E.P. Ricci, Nucl. Instrum. Methods 3 (1958) 223.
[27] N.N. Krot, M.S. Grigoriev, Russ. Chem. Rev. 73 (2004) 89.
[28] S.V. Krivovichev, Crystallogr. Rev. 10 (2004) 185.
[29] I.L. Botto, E.J. Baran, P.J. Aymonino, Z. Chemie 16 (1975) 163.
[30] B. Morosin, Acta Crystallogr. B34 (1978) 3732;
B. Morosin, Phys. Lett. A65 (1978) 53.
[31] A.N. Fitch, A.F. Wright, B.E.F. Fender, Acta Crystallogr. B38 (1982) 1108.
[32] A.N. Fitch, B.E.F. Fender, Acta Crystallogr. C39 (2) (1983) 162.
[33] A.N. Fitch, L. Bernard, A.T. Howe, A.F. Wright, B.E.F. Fender, Acta Crystallogr. C39 (2) (1983) 159.
[34] A.N. Fitch, M. Cole, Mater. Res. Bull. 26 (5) (1991) 407.
[35] A.J. Locock, P.C. Burns, M.J.M. Duke, T.M. Flynn, Can. Mineral. 42 (4) (2004) 973.
[36] A.J. Locock, P.C. Burns, T.M. Flynn, Can. Mineral. 42 (6) (2004) 1699.
[37] A.J. Locock, P.C. Burns, J. Solid State Chem. 177 (8) (2004) 2675.
[38] A.J. Locock, P.C. Burns, T.M. Flynn, Can. Mineral. 43 (2) (2005) 721.
[39] A.J. Locock, P.C. Burns, T.M. Flynn, Can. Mineral. 43 (2) (2005) 847.
[40] M. Rivenet, N. Vigier, P. Roussel, F. Abraham, J. Solid State Chem. 180 (2007) 713.
[41] F. Cesbron, N. Morin, Bull. Soc. Fr. Mineral. Cristallogr. 91 (5) (1968) 453.
[42] D.P. Shashkin, Dokl. Akad. Nauk SSSR 220 (6) (1975) 1410.
[43] P. Piret, J.P. Declerco, D. Wauters-Stoop, Bul. Mineral. 103 (2) (1980) 17.
[44] K. Mereiter, Neues jahrbuch fuer mineralogie, Monatshefte 12 (1986) 552.
[45] K.A. Hughes, P.C. Burns, U. Kolitsch, Can. Mineral. 41 (3) (2003) 677.